

REASSESSMENT OF THE AGE OF BASEMENT IN THE VAVILOV BASIN DRILLED AT ODP SITE 651 (TYRRHENIAN SEA, MEDITERRANEAN)

ISABELLA RAFFI^{*1} & AMALIA NOTARO²

¹International Research School of Planetary Sciences - IRSPS, Università degli Studi “G. d’Annunzio” di Chieti-Pescara, I-65127 Pescara, Italy.
E-mail: isabella.raffi@unich.it

²Dipartimento di Ingegneria e Geologia, Università degli Studi “G. d’Annunzio” di Chieti-Pescara, I-66013 Chieti Scalo, Italy.

*Corresponding author. Member of Editorial Board.

Associate Editor: Silvia Gardin.

To cite this article: Raffi I. & Notaro A. (2025) - Reassessment of the age of basement in the Vavilov Basin drilled at ODP Site 651 (Tyrrhenian Sea, Mediterranean). *Rivista Italiana di Paleontologia e Stratigrafia*, 131(1): 1-10.

Keywords: Calcareous nannofossils; biochronology; ODP Site 651; Tyrrhenian Sea; basement age.

Abstract: We carried out a biostratigraphic study based on calcareous nannofossils in sediments from Ocean Drilling Program (ODP) Site 651, drilled in the basalt-floored Vavilov sub-basin of the Tyrrhenian Sea (western Mediterranean) during Leg 107. The expedition achieved its primary objective to collect basement samples to date the ocean crust and obtain new data for reconstructing the geological evolution of the area. Studies on the ODP Site 651 succession determined the nature of the basement and provided time constraints for tectonic and magmatic processes in the basin, but contradictory lines of evidence emerged for the age of the basalts based on radiometric ages, paleomagnetic signature and planktonic foraminifera data. In an attempt to clarify the basement age, we performed detailed sampling for calcareous nannofossil analysis to update the biostratigraphy and chronology of the sediments overlying the basement. We determined the sediment accumulation rate using reliable nannofossil biohorizons that have a robust chronology, which increases up-section from ~ 2 cm/kyr to 3.4 cm /kyr. The age of the basalt/sediment contact was obtained through extrapolation of the sedimentation rate from the deepest datable portion of the sediments down to the top of basement. The inferred age for the top of the basalt is at least 4.1-4.2 Ma and differs from previous evaluations. This age for the basalt in the Vavilov Basin basement is consistent to a reversed interval C2Ar within the Gilbert magnetochron, supporting one of the chronologies previously proposed.

INTRODUCTION

In January-February 1986, the Ocean Drilling Program (ODP) Leg 107 drilled in the Tyrrhenian Sea (western Mediterranean) at seven sites (650 to 656) (Kastens, Mascle, Auroux et al. 1987) with the objective of providing timing constraints for tecto-

nic and magmatic processes in the basin and adding new information on the geologic evolution of the area. During the expedition, ODP Sites 650, 651 and 655 were drilled in two adjacent basalt-floored sub-basins of the Tyrrhenian Sea (Site 650 in the Marsili Basin, Sites 651 and 655 in the Vavilov Basin; Fig. 1) to obtain data on the nature of the basement and the timing of the development of the whole Tyrrhenian basin. At ODP Site 651, the primary objectives were achieved, including identifying the

nature of basement in the Vavilov Basin and dating the overlying sediments and the sediment/basalt contact (Kastens & Mascle 1990). Specifically, the basement turned out to be more complex and the sediment younger than had been anticipated. Moreover, the recovery of basement rocks consisting mainly of basalts overlying serpentized peridotite had important tectonic implications (Shipboard Scientific Party 1987; Bonatti et al. 1990; Kastens & Mascle 1990; Sartori 1990). However, the age of the basalts at Site 651 were problematic, due to discrepancy among the results derived from different methods (see discussion and notes in Kastens & Mascle 1990, and references therein). In fact, the radiometric ages obtained from $^{39}\text{Ar}/^{40}\text{Ar}$ dating the basalt were 3.0 to 2.6 Ma and pointed to a normal polarity interval of Chron C2An (Gauss), whereas the measured magnetic polarity of the basalts indicated a reversed interval (Vigliotti et al. 1990) that was correlated to either the bottom part of Chron C2r (Matuyama) (Subchron C2r.2r dated to 2.155 - 2.610 Ma; ages from Channell et al., 2020) or the upper part of Subchron C2Ar (upper part of the Gilbert, from 3.596 to 4.187 Ma). In addition, the presence of rare and poorly preserved planktonic foraminifera (*Globorotalia crassaformis*) was reported in a thin section from a dolostone fragment within the basement of Site 651 (Shipboard Scientific Party 1987, p. 310; Sartori 1990). This finding was considered compatible with either the Matuyama magnetostratigraphic interpretation or with the 3.0 to 2.6 Ma radiometric date (Kastens & Mascle 1990 and references therein), adding uncertainty to obtaining a reliable basement age. The sediment accumulation rate, inferred for the sediment section above the basement based on magnetostratigraphic and biostratigraphic results, was extrapolated down to the top of the basalt and suggested an age of 3.5 to 3.6 Ma for the sediment/basalt contact (Shipboard Scientific Party 1987). This age is consistent with the reversed interval at the top of the Gilbert magnetostratigraphic (Kastens & Mascle 1990), although the extrapolation was based on the “unsupported assumption that sedimentation rate in the red-brown basal sediments” was “the same as the overlying sediments” (Shipboard Scientific Party 1987; p. 326).

In the light of these different results for the age of the basement of the Vavilov Basin, it is surprising that in the past few decades there have been no updates to the biostratigraphy/chronology pu-

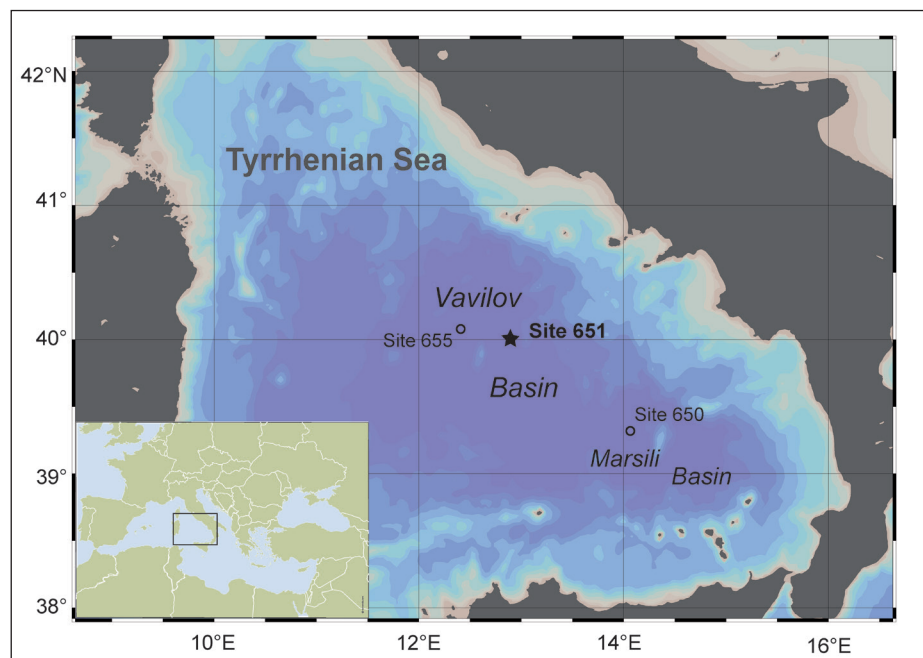
blished in the ODP Initial Reports and Scientific Results Volumes for Leg 107. Therefore, this study was developed to conduct a detailed biostratigraphic analysis, based on calcareous nannofossils, for ODP Site 651 with the aim of updating through biochronology the age of the sediments directly overlying the basement complex and possibly to support one of the suggested hypotheses on the age of the basement.

MATERIAL AND METHODS

At ODP Site 651 (Fig. 1), located at $40^{\circ} 09.03'$ N, $12^{\circ} 45.39'$ E at a water depth of 3578 m, a single hole (651A) was drilled to 551 m below sea floor (mbsf) with a highly variable recovery (from 2% to 100%) that resulted in ~ 190 m of core recovered. Most of the sedimentary section above the basement comprises volcanogenic sediments (volcaniclastic sands and breccias, pumice, lapilli tuff) interbedded with volumetrically subordinate (<15%) marly nannofossil ooze and turbiditic sediments, all assigned to “Sedimentary Unit I” (from 0 to 136 mbsf). “Sedimentary Unit II” (136 to 387 mbsf) was differentiated from Unit I by having a greatly reduced volcaniclastic component, finer grain size sediments, and increased clay and calcium carbonate content (Shipboard Scientific Party 1987).

We collected samples for calcareous nannofossil analysis from the lower part of “Sedimentary Unit II”, assigned to “Sub-unit IIa”, in the interval from 309.54 to 354.58 mbsf (Cores 651A-34R to 651A-38R) that mainly comprises calcareous lithologies (marly nannofossil ooze, chalk and calcareous claystone) with minor intercalations of tuffaceous clay and sapropelitic horizons. The sampled sediments overlie fragmented basaltic rocks that represent the local top of the basement, located at ~ 387 mbsf and which was penetrated downhole to 551 mbsf. The precise basalt/sediment contact was not recovered. The lowermost samples for this study, taken in Core 651A-38R, are from the upper part of the 40-m-thick “Sub-unit IIb” that consists of dolomite-rich sediments (“metalliferous dolostone” comprising dolomitic claystone, dolostone, and minor volcanic ash) immediately above the basement. We did not sample the pieces of pink dolostone recovered just above the first occurrence of basalt at 387.6 mbsf (Section 651A-42R-1), in which poorly

Fig. 1 - Location of ODP Sites 651 and 655 in the Vavilov Basin, the northwestern-most of the two deep sub-basins in the central Tyrrhenian Sea. The southwestern Marsili Basin is also shown with ODP Site 650 location. (Map modified from Schlitzer, Reiner, Ocean Data View, <http://odv.awi.de> 2022).



preserved planktonic foraminifera were observed (Shipboard Scientific Party 1987), because of the unsuitability of this lithology for preserving nanofossils.

We collected 71 samples from the ~ 45 m of sediments, with an average sampling resolution of 1 sample/63 cm. Sampling resolution varies depending on the intervals of drilling disturbance (in Cores 34R, 35R, 36R), and of scattered, though minor, intercalations of tuffaceous material, which were not samples. The samples were processed following the standard smear-slides procedure described by Bown & Young (1998).

Analyses of nanofossil assemblages were carried out using a light microscope Zeiss Axio-scope at 1200x magnification under cross-polarized and transmitted light. Photomicrographs of nanofossils were taken with the software “Image Pro Plus 7.0”. The entire composition of the assemblages was not quantitatively defined in detail, nor was the abundance of all the identified taxa evaluated. Instead, we only considered the biostratigraphic markers of the Late Pliocene to Early Pleistocene. Their abundance distribution was evaluated using semi-quantitative counting methods as follows: i) by counting the number of specimens in 30 fields of views of the smear slide, expressed as number per unit area (N/mm^2) (for all selected taxa except *Helicosphaera sellii*); ii) by counting the number of specimens of a species or morphotype vs. taxonomically related taxa, expressed as percentage. This latter

method was applied to evaluate large ($> 5.5 \mu m$) *Gephyrocapsa* spp. vs. all the *Gephyrocapsa* (medium and large) specimens and *H. sellii* vs. all the *Helicosphaera* specimens. The studied samples and numerical results for the selected taxa are reported in the *Appendix*.

For biostratigraphic classification we referred to the Neogene Mediterranean Zonation and biohorizon chronology recently published by Di Stefano et al. (2023).

BIOSTRATIGRAPHY AND CHRONOLOGY

The biostratigraphic results are given in Fig. 2, which shows the distribution ranges of zonal markers and additional taxa. The identified biohorizons are reported together with position of magnetic reversals (Channell et al. 1990) in Table 1. Although the magnetostratigraphy at Site 651 was disrupted by poor recovery and drilling disturbance, the main features of the Early Pleistocene/Late Pliocene polarity time scale were discerned (Channell et al. 1990; Table 1) within 32 m of the sediment succession. We compare our nanofossil results with this magnetostratigraphy below, in stratigraphic order.

Although the lowest part of the studied section in the dolomite-rich “Sub-unit IIb” above the basement (Core 6451A-38R) was “lithologically” unsuitable for finding microfossils, we collected and analyzed 12 samples in it. As expected, all of the

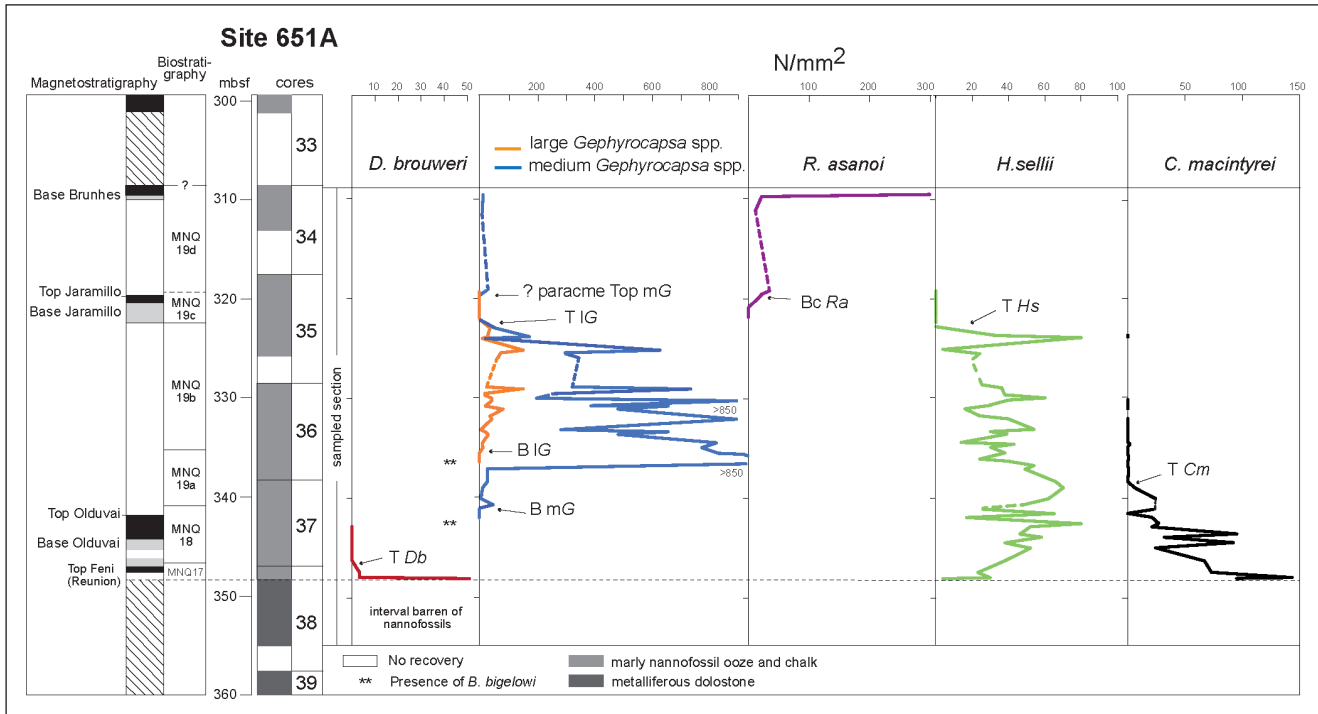


Fig. 2 - Abundance distribution patterns of selected calcareous nannofossils and their respective biohorizons that include: the biostratigraphic marker biohorizons (Top *D. brouweri* - T Db, Base medium *Gephyrocapsa* spp. - B mG, Base large *Gephyrocapsa* spp. - B IG, Top large *Gephyrocapsa* spp. - T IG) and the additional biohorizons (Top *Calcidiscus macintyrei* - T Cm, Top *Heliosphaera sellii* - T Hs, Paracme top medium *Gephyrocapsa* spp., Base common *Reticulofenestra asanoi* - Bc Ra). N/mm² = number of specimens per unit area of the smear slide.

se samples were barren of nannofossils except one from the top of the interval (651A-38R-1, 23 cm; 348.03 mbsf), in which a rich nannofossil assemblage was observed and ascribed to Zone MNQ17 (Di Stefano et al., 2023), based on the presence of *Discoaster brouweri* and *Discoaster triradiatus* (Plate 1). This result agrees with the shipboard nannofossil biostratigraphy for Site 651 (Shipboard Scientific Party 1987) that placed this interval in Zone NN18 of Martini (1971), which is equivalent to Zone MNQ17. The zone extends up to ~ 347 mbsf where the biohorizon Top *D. brouweri* (T Db) is placed and indicates an estimated age of 1.95 Ma that correlates with the base of Chron C2n (Olduvai) (1.925 Ma). The single scattered specimens of this taxon observed higher in the section (Core 651A-37) are considered reworked (see Appendix).

The favourable lithology and more continuous recovery of the sediments in Cores 651A-37R, 36R and part of Core 35R (from 348 to 319 mbsf), combined with higher resolution sampling, allowed us to obtain a more detailed biostratigraphy. Most of the samples have well preserved assemblages, although scattered samples are barren of nannofossils or have rare poorly preserved specimens

diluted by terrigenous or volcanic material. These samples, that are mainly from Core 651A-35R that contains dispersed layers of volcanic ash (Shipboard Scientific Party 1987), disrupt the biostratigraphy in the upper part of the studied section (Fig. 2). Despite this, the succession of biohorizons identified spans the Early Pleistocene time interval from 1.95 Ma to 0.95 Ma and includes Zones MNQ18 and MNQ19 (Di Stefano et al. 2023) (Fig. 2; Table 1). In addition to the biostratigraphic marker taxa we also identified specimens of *Braarudosphaera bigelowi* in discrete samples from Cores 651A-37R and 36R (Plate 1), which correspond to thin layers of sapropels described from these cores in the shipboard analyses (Shipboard Scientific Party 1987).

The first occurrence (Base) of medium-sized *Gephyrocapsa* spp. ($\geq 4 \mu\text{m}$ in size; Plate 1, figs. 6-8; B mG - 1.71 Ma) represents a distinct biostratigraphic horizon isochronously recorded worldwide (e.g., Raffi et al. 2006). This event is clearly delineated within the upper part of Core 651A-37R, just above the top of Chron C2n (Olduvai). “B mG” corresponds to the beginning of the evolutionary development that characterized the *Gephyrocapsa* genus through the Early Pleistocene interval, ex-

A. MAGNETOCHRON BOUNDARY	top sample	bottom sample	top depth (mbsf)	bottom depth (mbsf)	mid-point	Age (Ma)
Base C1n (Brunhes) *	34R-1, 6-8	34R-1, 17-19	309.37	309.48	309.42 ± 0.45	0.773
Top C1r.1n (Jaramillo)	35R-1, 66-68	35R-1, 130-132	319.57	320.21	319.89 ± 0.32	0.990
Base C1r.1n (Jaramillo)	35R-1, 130-132	35R-2, 148-150	320.21	321.89	321.05 ± 0.84	1.070
Top C2n (Olduvai) **	37R-3, 34-36	37R-3, 72-74	341.55	341.93	341.74 ± 0.19	1.770
Base C2n (Olduvai) **	37R-4, 146-148	37R-5, 108-110	344.16	345.29	344.72 ± 0.56	1.925
Top 2r.1n (Feni = Reunion)	37R-6, 52-54	37R-6, 134-136	346.23	347.05	346.64 ± 0.41	~ 2.100

B. BIOHORIZON	top sample	bottom sample	top depth (mbsf)	bottom depth (mbsf)	mid-point	Age (Ma)
Bc <i>Reticulofenestra asanoi</i>	35R-1, 74	35R-2, 49	319.63	320.89	320.26 ± 0.63	1.08
Top large <i>Gephyrocapsae</i> **	35R-3, 11	35R-3, 91	322.01	322.81	322.41 ± 0.40	1.24
Top <i>Helicosphaera sellii</i>	35R-3, 91	35R-4, 28	322.81	323.68	323.24 ± 0.43	1.26
Base large <i>Gephyrocapsae</i> **	36R-5, 28	36R-5, 84	334.88	335.44	335.16 ± 0.28	1.61
Top <i>Calcidiscus macintyrei</i>	37R-1, 12	37R-1, 72	338.32	338.92	338.62 ± 0.30	1.66
Base medium <i>Gephyrocapsae</i> **	37R-2, 93	37R-2, 140	340.63	341.10	340.86 ± 0.23	1.71
Top <i>Discoaster brouweri</i> **	37R-5, 77	37R-6, 55	344.97	346.25	345.61 ± 0.64	1.95

pressed in a trend of increasing size (Rio 1982; Raffi et al. 1993), and delineates Subzone MNQ19a (Di Stefano et al. 2023). The medium-sized *Gephyrocapsa* specimens show a rapid increase in abundance in the lower part of Core 651A-36R, above the final decline (Top) of *Calcidiscus macintyrei* (T *Cm* - 1.67 Ma) and is followed by the emergence of larger *Gephyrocapsa* specimens ($> 5.5 \mu\text{m}$; Plate 1, figs. 12, 13, 16) that defines the biohorizon “B1G” (1.61 Ma) and Subzone MNQ19b. The interval spanning the upper distribution range of the large *Gephyrocapsa* specimens (from the top of Core 651A-36R through Core 35R) is interrupted by the scattered volcanic/terrigenous material that diluted the nannofossil assemblages. Reworked taxa from the Paleogene and Neogene are present in greater abundance in samples from Cores 651A-34R and 35R than in the samples from the lower part of the section. The biohorizon Top large *Gephyrocapsa* spp. (T *lG* - 1.24 Ma), which defines the base of Subzone MNQ19c (Di Stefano et al. 2023), was delineated with a degree of uncertainty but its position is coherent with other biostratigraphic datums as it follows the disappearance (Top) of *H. sellii* (T *Hs* - 1.26 Ma) and precedes the biohorizons Base common *Reticulofenestra asanoi* (Bc *Ra* - 1.08 Ma) and paracme Top medium *Gephyrocapsa* spp. (paracme Top *mG* - 0.96 Ma) (although the latter biohorizon is not clearly delineated; Fig. 2). Comparison with paleomagnetic results shows that T *lG* (at ~ 322 mbsf) slightly precedes the recorded base of Subchron C1r.1n (Jaramillo) (at ~ 322 mbsf) and supports the assignment of this magnetic reversal to the Jaramillo (Channell et al. 1990).

These biostratigraphic results largely agree with previous time constraints based on paleomagnetic and planktonic foraminifera data (Shipboard Scientific Party 1987). The positions of nannofossil

Tab. 1 - A) Magnetochron boundaries for ODP Site 651 from Channell et al. (1990) and chronology from Channell et al. (2020). The samples which bracket the magnetozone boundaries are given. B) Positions of nannofossil biohorizons as delineated in the present study. The samples which bracket each biohorizon are given. Chronology from Di Stefano et al. (2023). Tie-points used for construction of sediment accumulation rates are indicated with asterisks: * from Shipboard Scientific Party (1987); ** this study.

biohorizons fit well with the original interpretation of the paleomagnetic data (Channell et al. 1990) except for at the top of the studied interval at top of Core 651A-34R, where there is a discrepancy between the magnetostratigraphic and biostratigraphic results and, consequently, in the age determination of that part of the section. Previous studies recorded the base of Chron C1n (Brunhes) between 309.37 and 309.48 mbsf (Shipboard Scientific Party 1987; Channell et al. 1990), which corresponds to an age of 0.773 Ma. By contrast, just below this depth (at 309.54 mbsf), in the topmost sample (651A-34R-1, 24 cm), the nannofossil data suggest an age at least 0.2 m.yr older than the age of 0.773 Ma provided by the magnetostratigraphic data. This older age estimate is supported by the presence of abundant specimens of *Reticulofenestra asanoi* in the nannofossil assemblage (Plate 1, figs. 14, 15), corresponding to a stratigraphic level well below the biohorizon Top common *R. asanoi* (the distinct decrease in abundance of the taxon) occurring at 0.90 Ma. Therefore, the recognized position of the Brunhes/Matuyama boundary is questionable.

We use this updated chronology to infer the accumulation rate of the sediments directly overlying the basement complex at Site 651, as discussed below. Note that differences with the previous chronology of the Site 651 sedimentary succession were expected due to the updates to the polarity time scale and, consequently, the updated ages of bioevents.

SEDIMENT ACCUMULATION RATES

As explained in the “Introduction”, evaluation of the sediment accumulation rate for the sedimentary succession just above the igneous basement

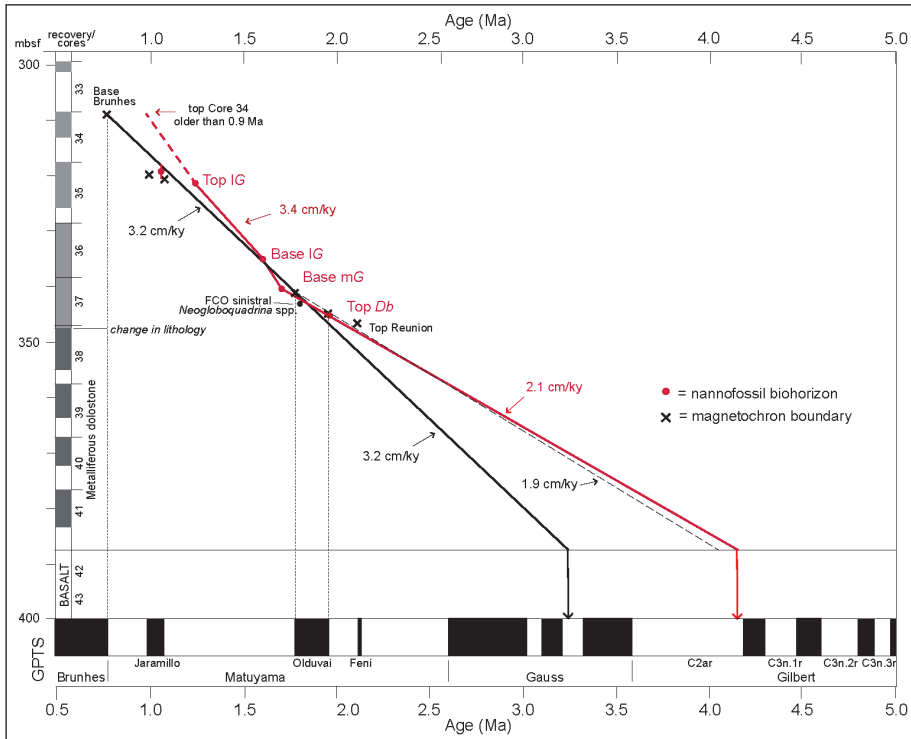


Fig. 3 - Sediment accumulation rate curves constructed between nannofossil biohorizons (red dots, lines, and rate in cm/kyr) and magnetochron boundaries (black crosses, lines, and rate in cm/kyr). Ages of magnetochrons from Channell et al. (2020) and from Global Polarity Time Scale – GPTS 2020 (Gradstein et al. 2020). Two options for the curve constructed from magnetochron boundaries are shown, one derived from original data (Shipboard Scientific Party 1987; solid line) the other from this study (dashed line).

was previously based on the chronology available at that time, which was derived from paleomagnetic and planktonic foraminifera data (Shipboard Scientific Party 1987). No correction for compaction of the sediments was applied. The different chosen tie-points were: i) the base of the Brunhes magnetochron; ii) the “Pliocene/Pleistocene boundary”, as recognized at that time by a planktonic foraminifera event (first common occurrence - FCO - of left-coiling *Neogloboquadrina pachyderma*) identified at Site 651 between 343.8 and 343.1 mbsf close to the top of the Olduvai magnetochron (~342 mbsf); and iii) the base of the Olduvai (at ~345 mbsf). The sediment accumulation rate was evaluated between the base Brunhes (at 310 mbsf) and the “Pliocene/Pleistocene boundary” (at ~343 mbsf), resulting in 3.3 cm/kyr; or between Base Brunhes and Base Olduvai (at 345 mbsf) resulting in 3 cm /kyr (Shipboard Scientific Party 1987, p. 303). After updating the ages for the tie-points base Brunhes (0.773 Ma), top and base Olduvai (1.770 and 1.925 Ma, respectively; ages from Channel et al. 2020) and FCO *Neogloboquadrina* spp. sinistral (1.79 Ma; Lirer et al. 2019) we obtained a similar sediment accumulation rate, on the order of 3.2 cm/kyr. Based on the assumption that sedimentation rate in the dolomitic basal sediments was the same as the overlying sediments (Shipboard Scientific Party 1987), we then extrapolated the sedimentation rate down to basement (at

~387 mbsf) and obtained an age of ~3.2 Ma for the basalt/sediment contact (Fig. 3). This result differs from the age of 3.5-3.6 Ma presented in the result volume of ODP leg 107 (Shipboard Scientific Party 1987; Kastens & Maslce 1990) because of the updated ages for polarity chrons.

For pursuing the aim of this study, we applied the methodology described above to evaluate the sediment accumulation rate using the more accurate chronology provided by calcareous nannofossils. As shown in Fig. 3, the inferred sediment accumulation rates slightly vary through the section, following an increasing trend from ~2 cm/kyr to 3.4 cm /kyr. As previously observed (Shipboard Scientific Party 1987), this increase reflects a gradual lithological change from mainly nannofossil ooze and chalk to marly nannofossil ooze with turbiditic sediments and minor intercalations of tuffaceous mud and clay.

The lowest portion of the sediment column datable by nannofossils is limited to a 4 m-interval (between ~341 mbsf and ~345 mbsf) that is bracketed by two reliable biohorizons, Base medium *Gephyrocapsa* spp. and Top *D. brouweri*. The ages for these tie-points, 1.71 Ma and 1.95 Ma, respectively, provide a sediment accumulation rate of 2.1 cm/kyr. Note that we obtained a similar result (1.9 cm/kyr) choosing the top and base Olduvai as tie-points for constructing the sediment rate curve (Fig. 3) in the lowest datable sediments. Extrapolating the se-

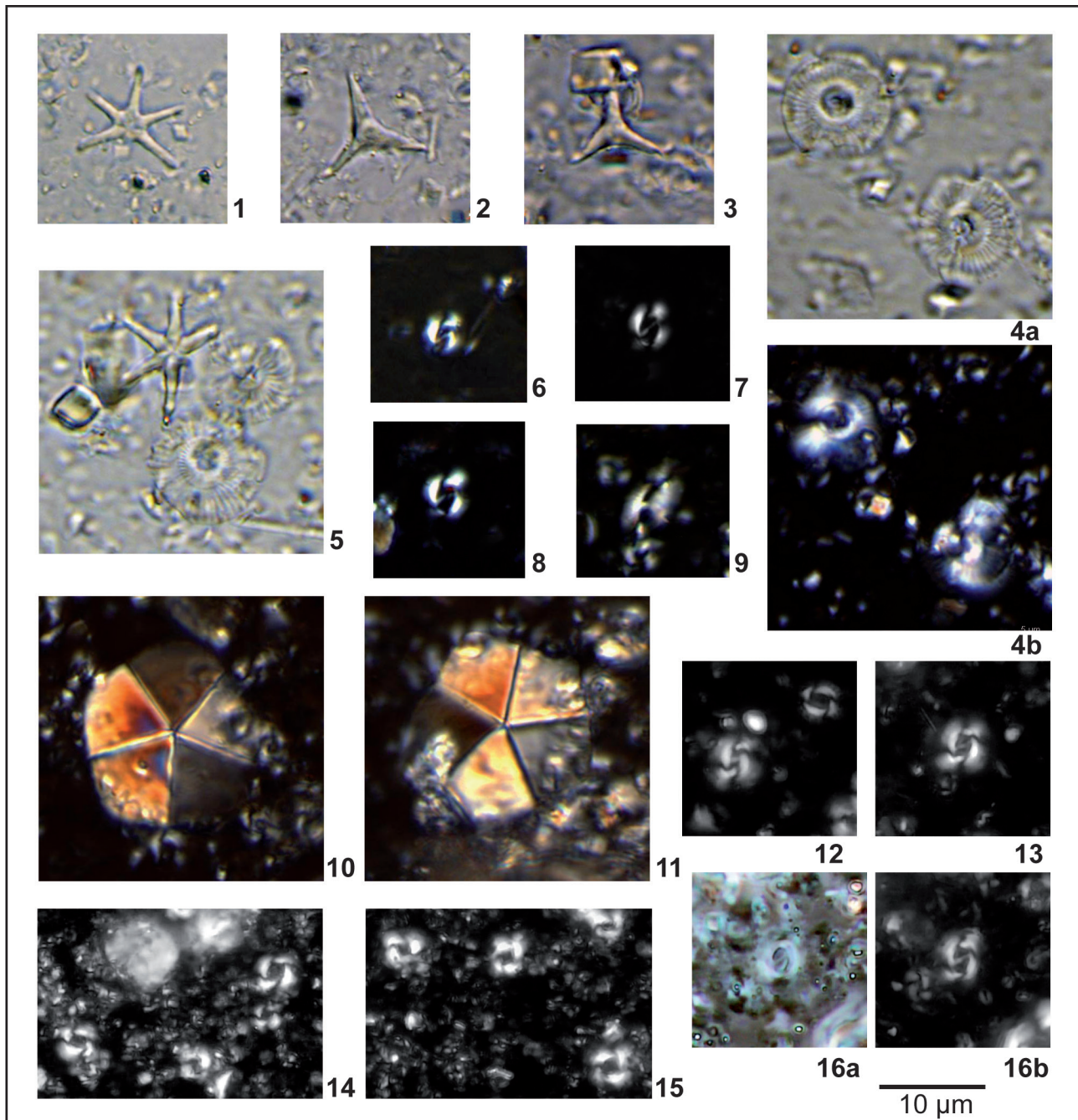


PLATE 1

Microphotographs of calcareous nannofossils from the ODP Leg 107, Site 651. All specimens X1200.

- 1) *Discoaster brouveri*, plane-transmitted light. Sample 107-651A-38R-1W, 23. 2, 3) *Discoaster triradiatus*, plane-transmitted light. Sample 107-651A-38R-1W, 23. 4a-4b) *Calcidiscus macintyrei*. Sample 107-651A-38R-1W, 23. 4a: plane-transmitted light; 4b: cross polarized light.
- 5) *D. brouveri* and *C. macintyrei*, plane-transmitted light. Sample 107-651A-38R-1W, 23. 6-8) medium *Gephyrocapsa* spp., cross polarized light. Sample 107-651A-36R-5W, 28. 9) *Helicosphaera sellii*, cross polarized light. Sample 107-651A-38R-1W, 23, 10, 11) *Braarudosphaera bigelovii*, cross polarized light. Sample 107-651A-37R-3W, 133. 12) medium *Gephyrocapsa* (5.5 μ m in size) and *Pseudoemiliania lacunosa*, cross polarized light. Sample 107-651A-35R-4W, 28. 13, 16a-16b) large *Gephyrocapsa* spp. (\geq 5.5 μ m in size), Sample 107-651A-35R-3W, 91; 16a: plane-transmitted light; 16b, 13: cross polarized light. 14, 15) Specimens of *Reticulofenestra asanoi*, cross polarized light. Sample 107-651A-34R-1W, 24.

dimentation rate from the lowest dated sediment down to the top basement at 387 mbsf (Fig. 3), we obtained an age of 4.1 - 4.2 Ma for the basalt/sediment contact.

This evaluation is tentative and possibly underestimated, given that i) the precise basalt/sediment contact location at Site 651 is uncertain; ii) correction for compaction of the sediments was not taken

651A Core				SECT	INT	mbsf	NANNOFOSSIL BIOSTRATIGRAPHY				<i>B. bigelovi</i>	<i>D. pentadactylus</i>	<i>D. brouweri</i> N/mm ²	<i>D. triradiatus</i> N/mm ²	<i>C. macintyrei</i> N/mm ²	<i>H. sellii</i> { % }	medium <i>Gephy</i> (N/mm ²)	large <i>Gephy</i> (N/mm ²)	large <i>Gephy</i> (%)	<i>Gephy</i> sp.3	<i>R. asanoi</i> (N/mm ²)
34	R	1	24			309.54										1	0	0		299	
34	R	1	46			309.76										13	0	0		0	
34	R	2	34			311.15	MNQ19c poor								1	0			0		
34	R	2	95			311.75													0	12	
35	R	1	30			319.2									X	X	19	X		35	
35	R	1	65			319.55										0	0	0		21	
35	R	1	74			319.63										0	0	0		22	
35	R	2	49			320.89									X	0	X	X		cf	
35	R	2	142			321.82										X	X	0		0	
35	R	2	146			321.86	B														
35	R	3	11			322.01										0	0	X		0	
35	R	3	45			322.35	B														
35	R	3	91			322.81										0	54	38	43		
35	R	4	28			323.68									X	33	175	28	22		
35	R	4	48			323.88									X	80	22	10	58		
35	R	4	132			324.22	B														
35	R	5	17			325.07										4	630	153	19		
35	R	5	62			325.52										24	299	76	20		
35	R	5	89			325.79	MNQ19c poor														
35	R	5	112			326.02										20	350	57	14		
36	R	1	14			328.74										0	25	325	25	17	
36	R	1	38			328.98									X	36	739	146	16		
36	R	1	54			329.14	B														
36	R	1	102			329.62	MNQ19b									0	38	242	19	20	
36	R	1	131			329.91										0	60	200	44	18	
36	R	2	6			330.16										0	40	898	43	13	
36	R	2	54			330.64									2	0	30	391	22	20	
36	R	2	59			330.69										0	30	659	21	7	
36	R	2	91			331.01										0	16	484	83	30	
36	R	3	12			331.72										0	24	770	38	5	
36	R	3	43			332.03										0	40	898	43	13	
36	R	3	138			333.08										0	54	286	6	1	
36	R	4	21			333.31										0	30	659	21	7	
36	R	4	44			333.54										0	39	484	31	6	
36	R	4	130			334.4										0	14	828	12	2	
36	R	4	145			334.55										2	43	817	11	2	
36	R	5	28			334.88										0	30	777	13	1	
36	R	5	84			335.44										0	38	834	0		
36	R	5	144			336.04										1	24	>800	0		
36	R	6	13			336.29										0	40	>800	0		
36	R	6	63			336.73										0	54	802			
36	R	6	96			337.06	MNQ19a									1	49	28			
37	R	1	12			338.32											0	66	28		
37	R	1	72			338.92										6	70	12			
37	R	2	34			340.04										24	62	6.4			
37	R	2	93			340.63									X	19	48	48			
37	R	2	103			340.73	MNQ19c poor														
37	R	2	140			341.1										22	26	0			
37	R	3	30			341.5										0	65	0			
37	R	3	71			341.91										21	17	0			
37	R	3	133			342.53									16		27	80			
37	R	4	14			342.84									X	0	0	21	52		
37	R	4	87			343.57	MNQ18									X	0	95	46		
37	R	4	120			343.9										0	0	32	58		
37	R	5	25			344.45										X	0	92	38		
37	R	5	77			344.97										0	0	24.5	52		
37	R	6	55			346.25										0	0	67	38		
37	R	7	22			347.42										3.2	2	73	23		
37	R	7	73			347.93	MNQ17									3.2	2	143	30		
38	R	1	23			348.03										51	16	95	4		
38	R	1	129			349.09	B														
38	R	2	136			350.66	B														
38	R	3	80			351.6	B														
38	R	3	110			351.9	B														
38	R	3	136			352.16	B														
38	R	4	11			352.41	B														
38	R	4	50			352.8	B														
38	R	4	110			353.4	B														
38	R	5	13			353.93	B														
38	R	5	54			354.34	B														
38	R	5	78			354.58	B														

B = barren of nannoosils

X = reworked specimens

APPENDIX

Appendix

Range chart of the selected taxa.

Numbers refer to the numerical results expressed as number of specimens per unit area (N/mm²) or percentage vs. related taxonomic group. "X" indicates presence that are due to reworking; "0" indicates that the absence of that taxon has been carefully checked. Greyish areas indicate barren samples or poorly preserved nannofossil assemblages.

into account; and iii) the same inferred rate has been assumed for both the calcareous ooze and the basal dolomitic sediments, even though the latter are more altered by diagenesis than the overlying ooze. Nevertheless, our inferred age of ~ 4.1 Ma suggests that the sediment/basement interface is within one of the reversed intervals of the Early Pliocene (C2ar or C3n.1r, C3n.2r, and C3n.3r of the C3n Gilbert polarity chron), thus supporting one of the options regarding the basement age (p. 25 in Kastens & Masclé 1990). From the biostratigraphic point of view, it is worth noting that the nannofossil results cast doubt on the presence of planktonic foraminifer *G. crassaformis* within the basement, a signal that was considered compatible with a “lower Matuyama magnetochron” age (Kastens & Masclé 1990). The fact that “*Globorotalia crassaformis* has been tentatively identified in thin section within the carbonate cement of a basalt breccia ...” (p. 326, Shipboard Scientific Party 1987) with very rare specimens observed in a thin section of such a lithologically unsuitable sediment, make the identification of that biostratigraphically useful foraminifer species poorly documented and questionable.

CONCLUSIONS

We conducted a detailed biostratigraphic study based on nannofossils of the sediments directly overlying the basement complex of the Vavilov Basin, allowing us to develop a new biochronology that permitted us to better constrain the age of that sediment section and, indirectly, the timing of the basaltic crust formation.

The importance of calcareous nannofossils in relative dating of marine sediments is well known, and the obtained robust biochronology has been used to identify which biohorizons can be used as reliable tie-points for inferring the sediment accumulation rate. The evaluated rate in the lowest datable portion of the sediment column (from ~ 341 mbsf to ~ 345 mbsf) is ~ 2 cm/kyr. Assuming that this inferred rate is the same in the basal dolomitic sediments, we extrapolated it down to the top of the igneous basement and obtained an age on the order of 4.1 – 4.2 Ma for the basalt/sediment contact. This evaluation is tentative, given the lack of information about compaction and diagenetic effects on the sediments. The inferred age for the top base-

ment fits with the evaluation obtained using updated magnetochron boundaries and ages as tie-points (top and base Olduvai) that are different from previous reconstruction (Shipboard Scientific Party 1987, fig. 15; Kastens & Masclé 1990). Our basement age correlates to a position within one of the Early Pliocene reversed intervals, occurring within Chron C3n (Gilbert) providing a support for one of the hypothesized time constraints of Vavilov Basin basement discussed in the report of Leg 107 results (Kastens & Masclé 1990). Moreover, our biostratigraphic results cast doubt on the identified position of the base of Chron C1n (Brunhes) at Site 651, probably related to ambiguous and discontinuous magnetostratigraphic signal and limited sample coverage (Shipboard Scientific Party 1987; Channell et al. 1990). Although we were not able to establish an age using nannofossils for the altered (dolomitized) sediments just above or within basement our data help to partially resolve the controversial results for the age constraints of Site 651 basalts.

Data Availability Statement

The data supporting the results of this research are available upon request. Interested researchers may contact the corresponding Author to obtain access.

Acknowledgments: This research used samples provided by the Integrated Ocean Drilling Program (IODP), sponsored by the U.S. National Science Foundation (NSF) and participating countries. Sampling was performed at the Bremen Core Repository - BCR - for IODP, ODP, DSDP cores with the helpful assistance of the repository staff. Technical support by the Department of Engineering and Geology, Università degli Studi “G. d’Annunzio” Chieti-Pescara is acknowledged. We are grateful to D. Kulhanek and an anonymous reviewer for their constructive comments and valuable input that improved the manuscript.

REFERENCES

- Bonatti E., Seyler M., Channell J.E.T., Giraudeau J. & Masclé J. (1990) - Peridotites drilled from the Tyrrhenian Sea, ODP Leg 107. In: Kastens K.A., Masclé J. et al. (Eds) - *Proceedings of ODP, Scientific Results*, 107: 37-47. College Station, TX (Ocean Drilling Program).
- Bown P.R. & Young J.R. (1998) - Techniques. In: Bown P.R. (Ed.) - *Calcareous Nannofossil Biostratigraphy*: 16-29. Kluwer Academic, Dordrecht.
- Channell J.E.T., Torii M. & Hawthorne T. (1990) - Magnetostratigraphy of sediments recovered at Sites 650, 651, 652, and 654 (Leg 107, Tyrrhenian Sea). In: Kastens K.A., Masclé J. et al. (Eds.) - *Proceedings of ODP, Scientific Results*, 107: 335-346. College Station, TX (Ocean Drilling Program).
- Channell J.E.T., Singer B. S. & Jicha B.R. (2020) - Timing of Quaternary geomagnetic reversals and excursions in volcanic and sedimentary archives. *Quaternary Science*

Reviews, 228, 106114. <https://doi.org/10.1016/j.quascirev.2019.106114>

Di Stefano A., Baldassini N., Raffi I., Fornaciari E., Incarbona A., Negri A., Bonomo S., Villa G., Di Stefano E. & Rio D. (2023) - Neogene-Quaternary Mediterranean calcareous nannofossil biozonation and biochronology: A review. *Stratigraphy*, 20(4): 259-302. <https://doi.org/10.29041/strat.20.4.02>

Gradstein F.M., Ogg J.G., Schmitz M.D. & Ogg G.M. (2020) - The Geologic Time Scale 2020: 1-1357. Elsevier, Amsterdam, Nederland.

Kastens K.A., Mascle J., Auroux C. et al. (1987) - Site 650: Marsili Basin. In: Stewart N.J. (Ed.) - *Proceedings of the ODP, Initial Reports Volume* 107: 129-285. College Station, Texas, Ocean Drilling Program.

Kastens K.A. & Mascle J. (1990) - The geological evolution of the Tyrrhenian Sea: an introduction to the Scientific Results of ODP leg 107. In: Kastens K.A., Mascle J. et al. (Eds) - *Proceedings of ODP, Scientific Results*, 107: 3-26. College Station, TX (Ocean Drilling Program).

Lirer F., Foresi L.M., Iaccarino S., Salvatorini G., Turco E., Cosentino C., Sierro F.J. & Caruso A. (2019) - Mediterranean Neogene planktonic foraminifer biozonation and biochronology. *Earth-Science Reviews*, 196: 102869.

Martini E. (1971) - Standard Tertiary and Quaternary calcareous nannoplankton zonation. In: Proceedings II Planktonic Conference, Roma: 739-785.

Raffi I., Backman J., Rio D. & Shackleton N.J. (1993) - Plio-Pleistocene nannofossil biostratigraphy and calibration to oxygen isotope stratigraphies from Deep Sea Drilling Project Site 607 and Ocean Drilling Program Site 677. *Paleoceanography*, 8: 387-408.

Raffi I., Backman J., Fornaciari E., Pälike H., Rio D., Lourens L. & Hilgen F. (2006) - A review of calcareous nannofossil astrobiochronology encompassing the past 25 million years. *Quaternary Science Reviews*, 25(23-24): 3113-3137. doi:10.1016/j.quascirev.2006.07.007.

Rio D. (1982) - The fossil distribution of Coccolithophore genus *Gephyrocapsa* Kamptner and related Plio-Pleistocene chronostratigraphic problems. In: Prell W. L., Gardner J. V. et al. (Eds) - *Initial Reports DSDP*, 68: 325-343. Washington (U.S. Govt. Printing Office).

Sartori R. (1990) - The main results of ODP Leg 107 in the frame of Neogene to recent geology of perityrrhenian areas. In: Kastens K.A., Mascle J. et al. (Eds) - *Proceedings of ODP, Scientific Results*, 107: 715-730. College Station, TX (Ocean Drilling Program).

Shipboard Scientific Party (1987) - 7. Site 651: Tyrrhenian Sea. Kastens, K.A., Mascle, J., Auroux, C., et al. (Eds) - *Proceedings of the ODP Program, Initial Reports Volume* (Pt. A), 107: 287-401. College Station, TX (Ocean Drilling Program).

Vigliotti L., Torii M. & Channell J.E.T. (1990) - Magnetic properties and paleomagnetism of basalts from Leg 107 (Holes 651A and 655B). In: Kastens K.A., Mascle J. et al. (Eds) - *Proceedings of ODP, Scientific Results*, 107: 99-110. College Station, TX (Ocean Drilling Program).